

Glass doped with semiconductor nanoparticles for optical devices

E. Rodriguez¹, L. Ponce¹; M. Arronte¹, E. de Posada¹, G. Kellerman², C. L. César³, and L. C. Barbosa³

¹INSTITUTO POLITÉCNICO NACIONAL; CICATA-UNIDAD ALTAMIRA-TAMAULIPAS; Km. 14.5 Carretera Tampico-Puerto Industrial Altamira; CP 89600; Altamira, Tamaulipas, México

²LNLS, R. Giuseppe Máximo Scolfaro, 10000, C.P. 6192 - CEP 13084-971 Campinas, SP, Brazil

³UNICAMP/IFGW/DEQ, CP 6165, CEP 13084-971, Barão Geraldo, Campinas, SP, Brazil.

ABSTRACT

We report the fabrication of glass multilayer doped with semiconductor nanoparticles. The glass matrix was fabricated by Plasma Enhanced Chemical Deposition (PECVD using tetramethoxysilane (TMOS) as precursor. The RF power was supplied by a RF-150 TOKYO HI-Power operating at 13.56 MHz and coupled to the RF electrodes through a matching box. The nanoparticles were grown by pulsed laser deposition (PLD) of a PbTe target using the second harmonic of a Q-Switched Quantel Nd:YAG laser in high purity inert gas atmosphere.

The influence of gas and background pressure and in the nanoparticle size and size distribution is studied. The morphological properties of the nanostructured material were studied by means of High Resolution Transmission Electron Microscopy (HRTEM), grazing-incidence small angle X-ray scattering (GISAXS)

Keywords: pulsed laser deposition, PECVD, Quantum Dots, Optical Device

1. INTRODUCTION

The study of semiconductor nanoparticles (NPs) embedded in glasses^[1] has attracted great attention because their non-linear optical properties^[2], making them promising materials for the development of integrated “all-optical” devices. However, their use has in many cases been hindered by the lack of appropriate deposition techniques with the capability to control the dimensions, shape, and size distribution of the NPs.

In this work we report the fabrication of glass multilayer doped with semiconductor NPs using alternatively Plasma Enhanced Chemical Vapor Deposition (PECVD) to grow the dielectric host and pulsed-laser deposition (PLD) to grow the PbTe NPs.

PbTe was chosen because its NPs absorption band can be controlled by its size to fall in the spectral window of interest for optical communications (1.3-1.5 μm). This, together with the QD high optical nonlinearity, makes this material an excellent candidate for development of optical devices.

PLD is a thin film deposition technique that has high potential for development of nanostructured materials. Once fixed the target-substrate distance, vacuum chamber pressure, and laser energy density, the QD size depends only on the amount of ablated material i.e. the number of laser pulses used to grow each QD layer. It means, that controlling the number of laser pulses one is able to control the QD size.

In order to produce NPs with absorption band in the infrared region, it is necessary to grow those nanoparticles with dimension from 6.5 to 8nm in diameter according to reports from Tudury et al^[3].

2. EXPERIMENTAL

Figure 1. shows the experimental set-up used for the fabrications of the nanostructures. It consists of a vacuum chamber pumped to a base pressure of $\sim 1 \times 10^{-7}$ mbar by a turbo molecular pump. Laser ablation of a PbTe target (99.99%) was performed using the second harmonic of a Q-Switched Quantel Nd:YAG laser. The pulse duration is 4 ns and the laser repetition rate is 20 Hz. The energy per pulse measured at the target surface was 70 mJ, which yields to a fluency of 20 J/cm². The pulsed laser beam is focused on an incidence angle of 45° on a target, using a 30 cm lens. The target holder can be rotated around the target normal, which reduces target degradation by multiple irradiation of a single spot.

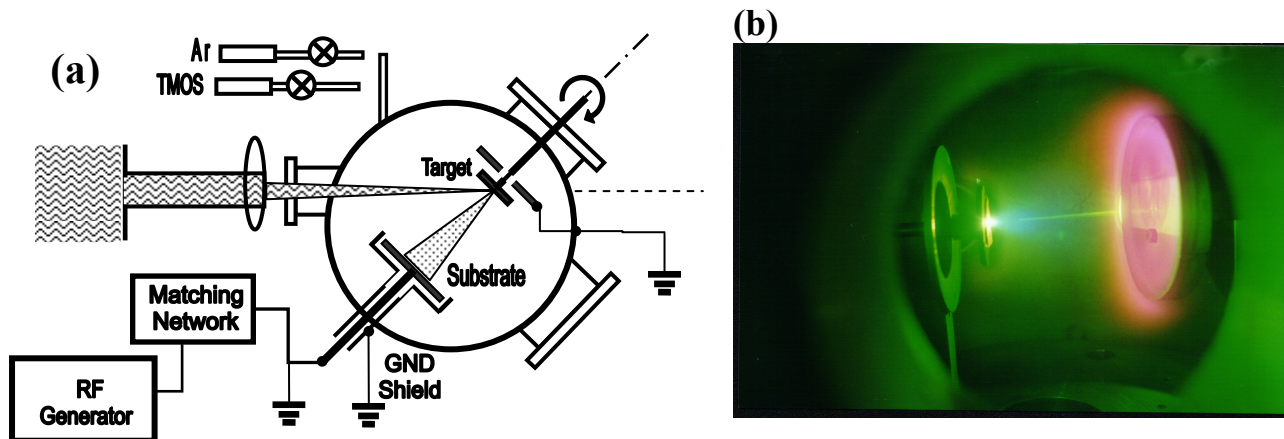


Figure 1: (a) Experimental set up used for the fabrication of the nanoparticles embedded in the dielectric matrix. The nanoparticles were grown by PLD of a PbTe target in argon atmosphere. The SiO₂ layer were grown by PECVD using TMOS as precursor. (b) plume produced by a laser pulse and plasma produced by de PECVD of TMOS

The source for the glass matrix is a silicon-alkoxide, tetrametoxysilane (TMOS). Vapor of TMOS evaporated in a vessel floated in a heat bath (30°C) was introduced into the chamber. Flow rate of both TMOS and Ar were controlled with independent flux controllers. Si(100) wafers or BK7 glass plates were used as substrates for HRTEM measurements and optical characterizations respectively. Substrate was maintained at room temperature. Multilayers were fabricated by alternatively PLD of the PbTe target during a time t_{LASER} and PECVD of TMOS during a time t_{RF} . A computer controlled interface switched properly RF and Laser Q-Switch. For optical characterization the above two-steps process is repeated several times until the amount of nanocrystals was enough to be measured. Total thickness of the nanostructured material can be controlled by changing the deposition time. Samples prepared for absorption measurements were grown about 1.5 μm thick. HRTEM was performed using a Jeol JEM 3010 microscope, 300kV and 1.7 Å point-to-point resolution. For optical characterization a lock in based experimental set up was used.

3. RESULTS AND DISCUSSIONS

3.1 X ray characterization of the glass doped with PbTe nanoparticles

The structural properties of the samples were studied using X-ray diffractometry. Figure 2 shows two typical diffractograms of the fabricated samples. Diffraction peaks corresponding to the (200) and (111) direction of the PbTe fcc structure can be seen in the diffractograms. According to Scherrer's method the QD diameter (Φ) can be calculated through the relation: $\Phi = \frac{k * \lambda}{\beta * \cos(\theta)}$, where $0.9 < k < 1$, λ is the wavelength, θ is the peak position and β is the peak FWHM. Using the diffraction peak located at $2\theta = 27.58^\circ$ ($\beta = 2.973^\circ$) corresponding to the (200) PbTe diffraction was possible to estimate the NPs size to 5 nm.

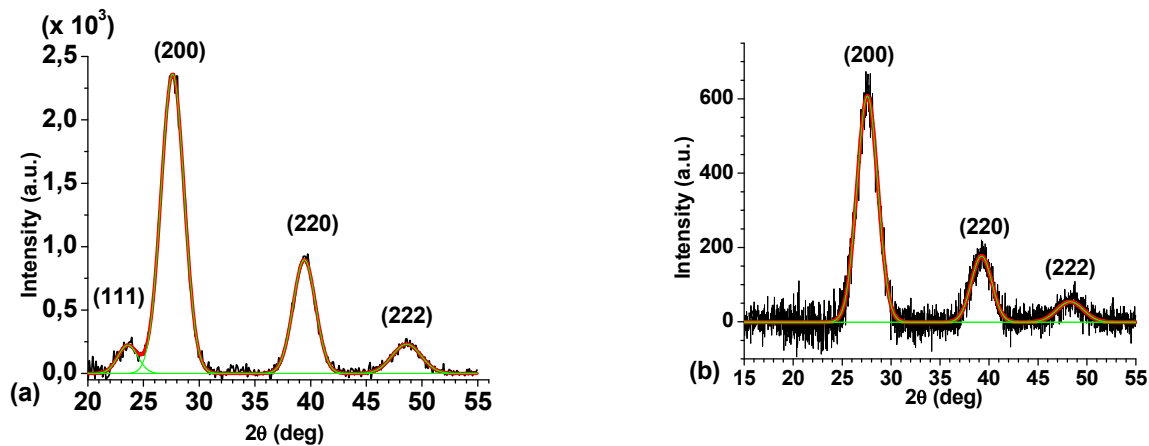


Figure 2: X-ray diffractograms of the SiO₂/PbTe multilayer. Measurements were carried out both in (a) grazing incidence (1.75°) and (b) $\theta:2\theta$ mode.

3.2 Characterization of the samples by grazing-incidence small-angle x-ray scattering (GISAXS)

To characterize the PbTe/SiO₂ multilayer structure, samples prepared under different growing conditions were studied by grazing-incidence small-angle x-ray scattering (GISAXS). The GISAXS intensity was measured as a function of the scattered momentum by using imaging-plate films. A schematic view of the setup used for GISAXS intensity measurements is given in Figure 3. A Huber four-circle diffractometer together with a phase scintillation detector from Cybestar were used in the study. Experiments were performed at the XRD2 x-ray diffraction beamline of the Brazilian Synchrotron Light Laboratory (LNLS) by using x-ray wavelength $\lambda = 1.5498 \text{ \AA}$.

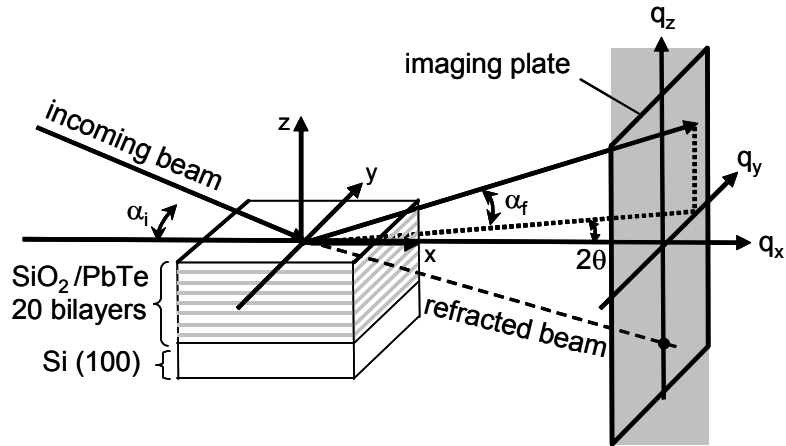


Figure 3: Schematic view of the experimental setup used for GISAXS experiments.

The two-dimensional GISAXS intensity pattern exhibit a set of stripes parallel to sample surface and regularly spaced in the vertical direction $q_z = 2\pi(\sin \alpha_i + \sin \alpha_f) / \lambda$, where α_i and α_f are the incidence and exit angle with respect to the sample surface, respectively. The GISAXS intensity from the A86 (100 RF pulses) sample is showed in Figure 4. The intensity associated to these stripes originates from the correlation between the roughness of multilayer interfaces giving rise to a resonant diffusely scattered (RDS) intensity.^{4,5,6} The maximums observed in reciprocal space occur at the lattice points of the one-dimensional reciprocal lattice of the multilayer. The distance of these stripes in the q_z direction is therefore $\Delta q_z = 2\pi / D$, where D is the multilayer period. The intensity profiles in the vertical direction as a function of scattering angle Figure 4(b) enabled the calculation of the multilayer period D .

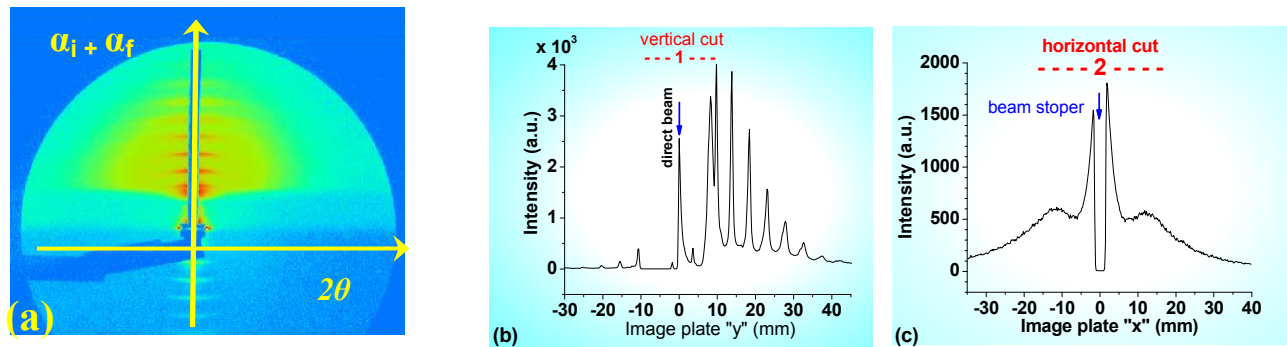


Figure 4: 2D GISAXS intensity image from PbTe/SiO₂ multilayer on Si (111). The non irradiated vertical stripe in the center of image is the shadow of the beamstopper used block the reflected and transmitted x-ray beams. (b) and (c) are typical figures obtained by cutting the two dimensional GISAXS pattern in the vertical and horizontal direction, respectively.

The GISAXS intensity in the vicinity of the specularly reflected beam is described by the distorted-wave Born approximation DWBA formalism, developed by Rauscher *et al.* [7]. As an approximation a gaussian function $N(R)$ was used to describe the radius distribution function of the PbTe NPs.

From the $N(R)$ function obtained by applying an appropriate fitting procedure to the whole set of scattering profiles Figure 5(a) at different q_z values, the nanocrystals average radius $\langle R \rangle$ and their relative radius dispersion $\sigma_R / \langle R \rangle$ were determined. Results show a continuous growth of the average radius $\langle R \rangle$ and a progressive increase in the radius dispersion σ_R (standard deviation of the $N(R)$ curves) of nanocrystals for increasing PbTe concentrations Figure 5(b), evidenced by a shift of the maximum of the distribution toward higher R 's and by the increasing full-width half-maximum of the $N_G(R)$ curves, respectively.

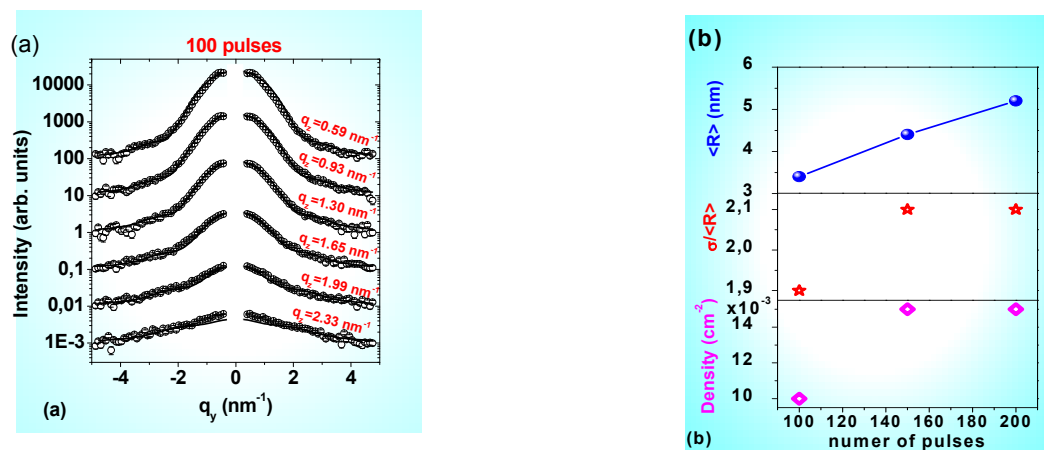


Figure 5: (a) GISAXS intensity profiles along the q_y for different q_z values, corresponding to the multilayer samples prepared with n_{LP} (PbTe)= 100. In order to avoid the intensity due the correlated interlayer interfaces (horizontally elongated spots in Fig. 4), the intensity profiles along q_y were chosen at q_z values localized between these maximums in which the contribution of the correlated intensity is expected to be negligible. The continuous lines are the best fit to the experimental data. (b) Dependence of the average nanoparticle size with the number of laser pulses.

3.2 Absorption measurements

The optical absorption measurements were done on the 1.5 μm thick SiO₂/PbTe structure. Even with this thickness the absorption was too weak to be detected with a single pass through the film, therefore we used a total internal reflection multipass arrangement for this measurement as shown in Figure 6(c). The experimental setup consisted of a 150 Watt halogen lamp mechanically chopped, a monochromator and a SR830 lock-in amplifier. The background spectrum was obtained with a SiO₂ film grown on the same substrate and with the same SiO₂ content as in the multilayer structure. Absorption bands clearly shift to lower wavelength when measurements were moved from position P to position R due to quantum confinement effects of the PbTe nanoparticles.

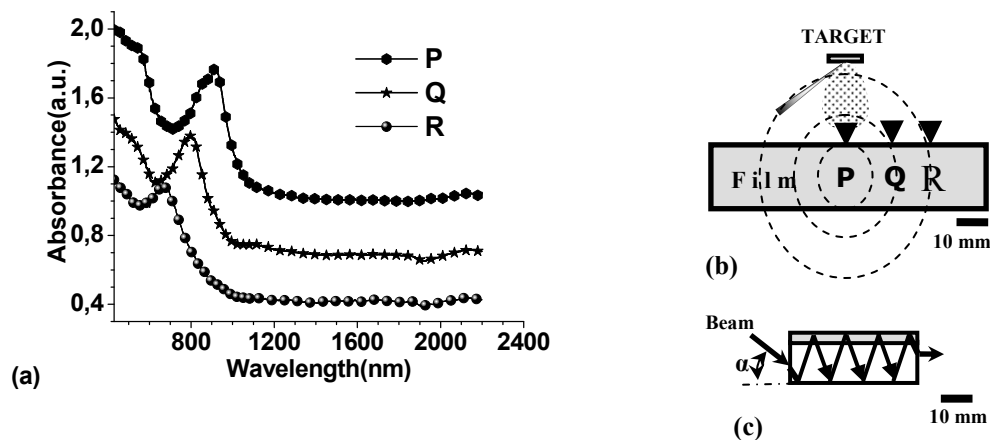


Figure 6 (a) Absorption spectra of a SiO_2/PbTe quantum dot multilayer grown by alternately PLD of PbTe nanoparticles and PECVD of SiO_2 . The measurements were carried out at three different sample regions P, Q and R (b), where the quantum dots have different sizes. Dashed rings are the isothickness contours corresponding to the in-plane distribution of the amount of PbTe deposited. (c) Schematic representation of the multiple pass total internal reflection geometry used for these measurements.

3.2 Characterization of the samples by transmission electron microscopy.

Figure 7 shows HRTEM images of two multilayer fabricated during the experiences reported in this work. Samples were prepared using the conventional sample preparation procedure. The ~ 25 nm amorphous layers between substrate and the first QD layer could be generated by the high power RF applied to substrate before the deposition of the first QD layer. This procedure was always used to improve the multilayer adherence to substrate.

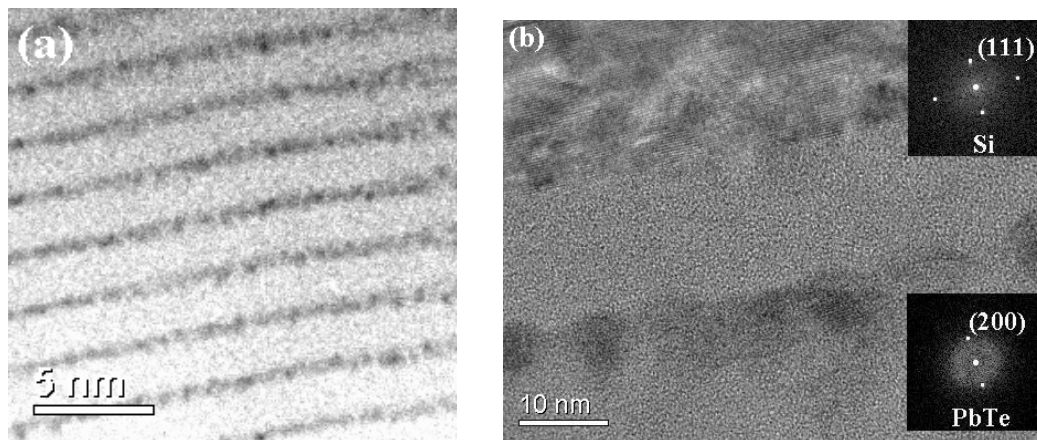


Figure 7 (a) cross-section image of a SiO_2/PbTe NPs structure fabricated in this work. Black layers correspond to PbTe nanoparticles separated by ~ 4 nm SiO_2 layers. For the complete structure 100 bilayers were deposited onto a Si(111) substrate. (b) High resolution image of a second multilayer fabricated during the experiences. In the HRTEM image can be appreciated the Si substrate (top) and the first QD layer (bottom). Insets showing the (111) diffraction for the Si substrate and the (200) diffraction for a PbTe nanoparticle. This micrograph shows ~ 6 nm thick QD layers.

4. CONCLUSIONS

A glass multilayer doped with PbTe nanoparticles was successfully fabricated by alternatively use of the PECVD and the PLD techniques. The influence of the amount of PbTe deposited on the size and size dispersion of the nanoparticles was studied by x-ray, GISAXS and HRTEM. Results show nanoparticles with diameters around 5 nm exhibiting absorption bans in the near infrared region.

5. AKNOWLEDGEMENTS

Authors thank Brazilian agencies CEPOF, PRONEX and FINEP for financial support. Dr. E. Rodriguez thanks São Paulo State Agency, FAPESP, under contract 04/06950-1 for financial support. Authors also gratefully thank Lab for Electronic Microscopy (LME) of the Brazilian Synchrotron Light Laboratory (LNLS) for the TEM measurements.

6. REFERENCES

-
- [1] Tsunetomo, K., Shunsuke, S., Koyama, T., Tanaka, S., Sasaki, F. and Kobayashi, S., "Ultrafast nonlinear optical response of CdTe microcrystallite-doped glasses fabricated by laser evaporation," *Molecular Crystals and Liquid Crystals Science and Technology Section B, Nonlinear Optics*, 13(1-3), 109-126 (1995)
 - [2] Gleiter, H., "Nanocrystalline Materials," *Prog. Mater. Sci.* 33, 223-315(1989)
 - [3] Tudury, G.E., Marquezini, M. V., Ferreira, L. G., Barbosa, L.C., and Cesar C.L., "Effect of Band Anisotropy on Electronic Structure of PbS, PbSe, and PbTe Quantum Dots," *Phys. Rev. B*, 62(11), 7357-64 (2000)
 - [4] Holý, V., and Baumbach, T., "Non specular x-ray reflection from rough multilayers," *Physical Review B* 49, 10668-10676(1994)
 - [5] Kortright, J. B., "Nonspecular X-ray scattering from multilayer structures," *J. Appl. Phys.* 70(7), 3620-3625 (1991)
 - [6] Jiang, X., Metzger, T. H. and Peisl, " Nonspecular x-ray scattering from the amorphus state in W/C multilayers," *Appl. Phys. Lett.* 61(8), 904-906 (1992)
 - [7] Rauscher, M., Paniago, R., Metzger, H., Kovats, Z., Domke, J. and Peisl, J., "Grazing incidence small angle x-ray scattering from free-standing nanostructures," *J. Appl. Phys.* 86, 6763 (1999).